

RESEARCH

Open Access



# Dysfunctional bone marrow endothelial progenitor cells are involved in patients with myelodysplastic syndromes

Tong Xing<sup>1,2</sup>, Zhong-Shi Lyu<sup>1,2</sup>, Cai-Wen Duan<sup>3</sup>, Hong-Yan Zhao<sup>1</sup>, Shu-Qian Tang<sup>1</sup>, Qi Wen<sup>1</sup>, Yuan-Yuan Zhang<sup>1</sup>, Meng Lv<sup>1</sup>, Yu Wang<sup>1</sup>, Lan-Ping Xu<sup>1</sup>, Xiao-Hui Zhang<sup>1</sup>, Xiao-Jun Huang<sup>1,2</sup> and Yuan Kong<sup>1\*</sup> 

## Abstract

**Background:** Myelodysplastic syndromes (MDS) are a group of heterogeneous myeloid clonal disorders characterized by ineffective haematopoiesis and immune deregulation. Emerging evidence has shown the effect of bone marrow (BM) endothelial progenitor cells (EPCs) in regulating haematopoiesis and immune balance. However, the number and functions of BM EPCs in patients with different stages of MDS remain largely unknown.

**Methods:** Patients with MDS (N = 30), de novo acute myeloid leukaemia (AML) (N = 15), and healthy donors (HDs) (N = 15) were enrolled. MDS patients were divided into lower-risk MDS (N = 15) and higher-risk MDS (N = 15) groups according to the dichotomization of the Revised International Prognostic Scoring System. Flow cytometry was performed to analyse the number of BM EPCs. Tube formation and migration assays were performed to evaluate the functions of BM EPCs. In order to assess the gene expression profiles of BM EPCs, RNA sequencing (RNA-seq) were performed. BM EPC supporting abilities of haematopoietic stem cells (HSCs), leukaemia cells and T cells were assessed by in vitro coculture experiments.

**Results:** Increased but dysfunctional BM EPCs were found in MDS patients compared with HDs, especially in patients with higher-risk MDS. RNA-seq indicated the progressive change and differences of haematopoiesis- and immune-related pathways and genes in MDS BM EPCs. In vitro coculture experiments verified that BM EPCs from HDs, lower-risk MDS, and higher-risk MDS to AML exhibited a progressively decreased ability to support HSCs, manifested as elevated apoptosis rates and intracellular reactive oxygen species (ROS) levels and decreased colony-forming unit plating efficiencies of HSCs. Moreover, BM EPCs from higher-risk MDS patients demonstrated an increased ability to support leukaemia cells, characterized by increased proliferation, leukaemia colony-forming unit plating efficiencies, decreased apoptosis rates and apoptosis-related genes. Furthermore, BM EPCs induced T cell differentiation towards more immune-tolerant cells in higher-risk MDS patients in vitro. In addition, the levels of intracellular ROS and the apoptosis ratios were increased in BM EPCs from MDS patients, especially in higher-risk MDS patients, which may be therapeutic candidates for MDS patients.

\*Correspondence: successky@163.com

<sup>1</sup> Peking University People's Hospital, Peking University Institute of Hematology, National Clinical Research Center for Hematologic Disease, Beijing Key Laboratory of Hematopoietic Stem Cell Transplantation, Collaborative Innovation Center of Hematology, Peking University, Beijing, China  
Full list of author information is available at the end of the article



© The Author(s) 2022. **Open Access** This article is licensed under a Creative Commons Attribution 4.0 International License, which permits use, sharing, adaptation, distribution and reproduction in any medium or format, as long as you give appropriate credit to the original author(s) and the source, provide a link to the Creative Commons licence, and indicate if changes were made. The images or other third party material in this article are included in the article's Creative Commons licence, unless indicated otherwise in a credit line to the material. If material is not included in the article's Creative Commons licence and your intended use is not permitted by statutory regulation or exceeds the permitted use, you will need to obtain permission directly from the copyright holder. To view a copy of this licence, visit <http://creativecommons.org/licenses/by/4.0/>. The Creative Commons Public Domain Dedication waiver (<http://creativecommons.org/publicdomain/zero/1.0/>) applies to the data made available in this article, unless otherwise stated in a credit line to the data.

**Conclusion:** Our results suggest that dysfunctional BM EPCs are involved in MDS patients, which indicates that improving haematopoiesis supporting ability and immunoregulation ability of BM EPCs may represent a promising therapeutic approach for MDS patients.

**Keywords:** Myelodysplastic syndromes, Endothelial progenitor cells, Haematopoiesis, Immune regulation

## Background

Myelodysplastic syndromes (MDS) refer to a group of heterogeneous myeloid clonal disorders characterized by abnormal development of myeloid cells, which manifest as ineffective haematopoiesis and a tendency to transform into acute myeloid leukaemia (AML) [1–3]. The pathogenesis of MDS is complex and diverse and includes inherent genetic abnormalities in myeloid progenitor cells, changes in the bone marrow (BM) microenvironment, and chronic immune stimulation [1, 4, 5]. Current strategies to treat MDS rely on allogeneic haematopoietic stem cell transplantation (allo-HSCT), hypomethylating agents, immunosuppressive therapy and chemotherapy [6–9], which have not achieved satisfactory clinical efficacy [10, 11]. Taking allo-HSCT as an example, only 40 to 50% of patients survive for 5 years [12, 13]. Therefore, further study of MDS pathogenesis is urgently needed to provide new treatment strategies for MDS patients.

The growth and spread of malignant clones represent the dominant pathophysiological process of MDS [14, 15]. With disease progression, malignant cells gradually replace normal haematopoietic stem cells (HSCs) and eventually dominate the BM [16, 17]. Progression of MDS to AML is thought to result from a shift from apoptosis to proliferation of these malignant clones [18]. As another important pathogenic mechanism of MDS, immune deregulation has been shown in a great number of MDS patients [19, 20]. For example, T helper (Th) 17 cells were increased in lower-risk MDS, and regulatory T cells (Tregs) were increased in higher-risk MDS [21, 22], which suggests that progression is facilitated by immune suppression. Therefore, understanding the mechanisms of ineffective haematopoiesis and immune deregulation in MDS patients is of considerable importance.

Emerging evidence has shown important roles of the BM microenvironment in regulating haematopoiesis and immune balance [23–25]. Previous murine studies [24, 26, 27] and our previous studies [28–30] have reported that endothelial progenitor cells (EPCs) are an important component of the normal BM microenvironment to support HSCs. However, Sophia et al. reported that increased BM EPCs may contribute to inferior haematopoietic function in a MDS murine model [31]. In vitro experiments have shown a poor ability of endothelial colony forming cells from the peripheral blood of MDS patients to support HSCs [32]. These evidences suggest

that EPCs demonstrate inferior supporting ability to normal HSCs in MDS whereas the supporting abilities in patients with different stages of MDS remain to be comprehensively depicted. In terms of malignant cells, intrinsic apoptotic signals like clonal chromosomal changes or gene mutations contribute to progression to AML [16]. However, extrinsic apoptotic signals which are related to immune and microenvironment are also considered the pivotal reasons of the transformation of clonal progenitors from MDS to AML [1]. Mice transplantation experiment proved that leukemia-derived endothelial cells are capable of giving rise to AML in normal mice [33]. However, the supporting abilities of BM EPCs to malignant cells in MDS remain unclear. Furthermore, although normal human EPCs exhibit immunosuppressive properties [34–36], the immunomodulatory effect of BM EPCs has not been reported in MDS patients.

Therefore, the current study was performed to explore the functions of BM EPCs in MDS patients, including lower-risk MDS and higher-risk MDS patients. The number and functions of BM EPCs from MDS patients, de novo AML patients and healthy donors (HDs) were analysed. Bulk RNA sequencing (RNA-seq) was used to further explore the expression profile of BM EPCs, and in vitro coculture strategies were used to evaluate the abilities of BM EPCs to regulate haematopoiesis and immunity. Our aim was to provide a potential therapeutic strategy for MDS patients.

## Methods

### Patients and controls

Patients with MDS (N=30) and de novo AML (N=15) were enrolled. Newly diagnosed MDS patients (N=30) were divided into lower-risk MDS (N=15) and higher-risk MDS (N=15) groups (Additional file 1: Table S1) according to the dichotomization of the Revised International Prognostic Scoring System (IPSS-R) [37]. AML patients were diagnosed with de novo M2 (N=8), M4 (N=2) or M5 (N=5) disease [38]. Bone marrow cells from allogeneic transplantation donors (N=15) were used as normal controls. The age of lower-risk MDS (51.3 years, range 29–69), higher-risk MDS (48.4 years, range 24–68), AML (51.2 years, range 26–64) patients and HDs (49.5 years, range 29–64) showed no significant differences.

### Isolation, cultivation, and characterization of primary BM EPCs

As previously reported [28–30, 39, 40], BM mononuclear cells (BMMNCs) were isolated by density gradient centrifugation using lymphocyte separation medium (GE Healthcare, Milwaukee, USA). Precultivated BM EPCs were characterized by staining with mouse anti-human CD45 (BD Biosciences, San Jose, USA), CD34 (BioLegend, San Diego, USA), CD133 (Miltenyi Biotec, Bergisch Gladbach, Germany), and vascular endothelial growth factor receptor 2 (VEGFR2, CD309) monoclonal antibodies (BD Biosciences, San Jose, USA). Data were analysed with BD FACSDIVA v8.0 Software (BD Biosciences).

BMMNCs ( $5 \times 10^6$  per well) were cultured in fibronectin-precoated (Sigma, St. Louis, USA) 6-well culture plates with EGM-2-MV-SingleQuots (Lonza, Walkersville, USA) and 10% foetal bovine serum (FBS; Gibco, Australia) at 37 °C in a humidified incubator with 5% CO<sub>2</sub> for 7 days until testing.

BM adherent cells at day 7 of cultivation were further functionally characterized as BM EPCs for their capacity to uptake Acetylated low-density lipoprotein (AcLDL) and to bind Ulex europaeus agglutinin I (UEA I) [28–30, 40, 41]. The adherent cells were incubated with DiI-AcLDL (Life Technologies, Gaithersburg, USA) at 37 °C. After 4 h, the cells were fixed with 4% prechilled paraformaldehyde and incubated with 10 µg/ml fluorescein isothiocyanate-labeled UEA I (FITC-UEA I; Sigma, St. Louis, USA) for 1 h. To evaluate the numbers of double-positive-stained EPCs, three power fields were randomly counted using a fluorescence microscope (Olympus, Tokyo, Japan).

After 7 days of cultivation, EPC identity was confirmed by real-time quantitative polymerase chain reaction (qRT-PCR) for endothelial specific marker genes (VEGFR2, VE-cadherin and vWF) [41, 42].

### Tube formation and migration assays

A total of  $4 \times 10^4$  EPCs at day 7 of cultivation were transferred to matrigel-coated (Corning, New York, USA) plates and incubated for 48 h at 37 °C in 5% CO<sub>2</sub>. Tube formation [28, 29, 39, 40] was measured by determining the relative tube length per field of view using an inverted light microscope. All cells were counted in three random fields.

Cell migration [28–30, 39, 40, 43] was assayed using a transwell chamber (Corning, New York, USA). The EPCs after 7 days of culture were seeded in the upper chambers at a density of  $4 \times 10^4$  cells per well, while 500 µl medium was added to the lower chamber. The cells were cultured for 24 h, and migrated cells were fixed with paraformaldehyde for 30 min. Then, cells on

the bottom surface of the membrane were stained with crystal violet for 20 min and counted manually in three random fields/sample. Cell images were obtained on a phase-contrast microscope (Olympus, Tokyo, Japan).

### HSCs, T cells or HL-60 cells were cocultured with BM EPCs

In order to evaluate the effect of supporting ability of BM EPCs to normal HSCs, T cells or HL-60 cells, the cultivated BM EPCs from HDs or MDS or AML patients were cocultured with normal CD34<sup>+</sup> cells, or normal CD3<sup>+</sup> cells, or HL-60 cells [28–30, 40, 44]. HSCs or T cells were isolated from BMMNCs of HDs using CD34 or CD3 MicroBead kits (Miltenyi Biotec, Bergisch Gladbach, Germany). Cultivated EPCs (described before) were plated onto gelatinized 24-well culture plates at  $1 \times 10^5$  cells/well and cultured overnight to achieve confluence. Then, HSCs ( $1 \times 10^5$  per well) or T cells ( $1 \times 10^5$  per well) or HL-60 cells (Manassas, Virginia, USA;  $5 \times 10^4$  per well) were added in direct contact with confluent and adherent EPCs. EPC-HSC cocultures were maintained in StemSpan™ SFEM (Stem Cell Technologies, Vancouver, Canada) for 5 days. EPC-T cells or HL-60 cells cocultures were maintained in RPMI 1640 medium supplemented with 10% FBS for 3 days or 5 days. Appropriate controls of T cell culture alone were also included.

### Intracellular reactive oxygen species (ROS) levels

To detect ROS levels of HSCs and precultivated EPCs [28, 29, 40], HSCs were stained with CD34, and BMMNCs were stained with the aforementioned EPC markers and incubated with 10 µM 2',7'-dichlorofluorescein diacetate (DCFH-DA, Byotime, Shanghai, China) at 37 °C for 15 min. All data were analysed on BD FACSDIVA v8.0 Software (BD Biosciences).

To detect ROS levels on day 7 of cultivated BM EPCs, adherent cells were incubated with 1 µg/ml DCFH-DA at 37 °C for 20 min. Images were obtained in three random fields/sample using a fluorescence microscope (Olympus, Tokyo, Japan). The fluorescence intensity of ROS was analysed via the mean grey value using ImageJ 1.52v (National Institutes of Health, Bethesda, USA).

### Apoptosis ratio analysis

To detect the apoptosis ratio, HSCs, precultivated EPCs or HL-60 cells were incubated with Annexin-V (BioLegend, San Diego, USA) and 7-amino-actinomycin D (7-AAD; BD Biosciences, San Jose, USA) for 10 min at room temperature and then analysed on BD FACSDIVA v8.0 Software (BD Biosciences).

### Colony-forming unit (CFU) and leukaemia colony-forming unit (CFU-L) assays

CFUs were assayed using MethoCult™ H4434 Classic (Stem Cell Technologies, Vancouver, Canada). After 5 days of coculture,  $2 \times 10^3$  CD34<sup>+</sup> cells or  $2 \times 10^3$  HL-60 cells were plated in 24-well plates and cultured for 14 days. Colony-forming unit erythroid (CFU-E), burst-forming unit erythroid (BFU-E), colony-forming unit-granulocyte/macrophages (CFU-GM), and colony-forming unit-granulocyte, erythroid, macrophage and megakaryocyte (CFU-GEMM) measurements for CD34<sup>+</sup> cells [28, 30, 44] and CFU-L measurements for HL-60 cells [45] were scored.

### Analysis of T cell subsets

After 3 days of coculture, CD3<sup>+</sup> T cells were stimulated with a cell stimulation cocktail (eBioscience, San Diego, USA) to induce CD3<sup>+</sup> T cell activation and cytokine secretion. Lymphocyte subpopulations were quantified via flow cytometry as previously described [46–49]. Th1, Th2, Th17 cells, and Tregs were identified as CD3<sup>+</sup>CD8<sup>-</sup>IFN- $\gamma$ <sup>+</sup>, CD3<sup>+</sup>CD8<sup>-</sup>IL-4<sup>+</sup>, CD3<sup>+</sup>CD8<sup>-</sup>IL-17A<sup>+</sup>, and CD3<sup>+</sup>CD8<sup>-</sup>CD25<sup>+</sup>Foxp3<sup>+</sup> populations, respectively. The details of antibodies were in Additional file 1: Table S2.

### 5-Ethynyl-20-deoxyuridine (EdU) assay

HL-60 cells were harvested after coculture with EPCs and then incubated with 50  $\mu$ M EdU (RiboBio, Guangzhou, China) in 48-well plates for 1 h at 37 °C. Then, according to the manufacturer's instructions, the nuclear fluorescence intensity was analysed on BD FACSDIVA v8.0 Software (BD Biosciences).

### RNA-seq and data analysis

RNA-seq analyses were performed to analyse the 7-day cultivated BM EPCs from HDs, lower-risk

MDS, higher-risk MDS or AML patients. The accession number of whole transcriptome RNA-seq data is GSE197907. Differential gene expression (DEGs), principal component analysis (PCA), hierarchical clustering analysis and Kyoto Encyclopedia of Genes and Genomes (KEGG) enrichment plot were executed by the DESeq2, clusterProfiler, pheatmap, and ggplot2 packages in R (1.16.1). The top 20 up and down regulated genes in higher-risk MDS BM EPCs than lower-risk MDS BM EPCs were list in Additional file 1: Table S3 and in AML BM EPCs than higher-risk MDS BM EPCs were list in Additional file 1: Table S4. Gene set enrichment analysis (GSEA) analysis was performed with respect to MSigDB (version 5.1) genesets C5 GO biological processes [50].

### qRT-PCR

For qRT-PCR, RNA was extracted using the RNeasy Mini kit (QIAGEN, Dusseldorf, Germany). One microgram of RNA was reverse transcribed into cDNA by the RT reagent Kit with gDNA Eraser (TaKaRa, Otsu, Japan). The mRNA levels of *VEGFR2*, *VE-cadherin*, *VWF*, *CASP2*, *CASP3*, *BAX*, *CCNE1*, *MCL1*, *TP53*, *CDKN1A*, *CXCL12*, *KITLG*, *NFKB1*, *HAVCR2*, *CIITA*, and *LGALS9* were detected by the SYBR-Green qRT-PCR kit (Thermo Fisher Scientific, Waltham, USA). The levels of the aforementioned genes were evaluated after normalization to the *18S* mRNA level [30]. All sequences of primers were list in Additional file 1: Table S5.

### Statistical analysis

Analyses were performed using GraphPad Prism 6.0. Statistical analyses were performed using Mann–Whitney U test. The relative mRNA analyses and paired analyses were using Wilcoxon matched-pairs signed rank test. The results are expressed as the means  $\pm$  SEM, and *P*-values < 0.05 were considered statistically significant.

(See figure on next page.)

**Fig. 1** The number and functions of BM EPCs from patients with MDS, HD and patients with de novo AML were enrolled as controls. **A, left** The EPC phenotype was characterized by demonstrating positive expression of CD34, CD309 and CD133 by flow cytometry. The **A, right** percentage of BM EPCs in precultivated BMMNCs was analysed. **B** Representative images (scale bars represent 200  $\mu$ m) of typical cultured BM EPCs collected at day 7 of culture from HDs and L-MDS, H-MDS and AML patients were characterized by double-positive staining (merged in yellow) with Dil-AcLDL (red) and FITC-UEA I (green) (original magnification, 10 $\times$ ). **C** Quantification of double-positive EPCs/field of view (merged in yellow) stained with Dil-AcLDL (red) and FITC-UEA I (green) at day 7 of culture (original magnification, 10 $\times$ ). **D** Representative images (scale bars represent 200  $\mu$ m) of tube formation (pixels of tubes per field of view) by BM EPCs at day 7 of culture (original magnification, 10 $\times$ ). **E** Quantification of tube length (pixels of tubes per field of view) of BM EPCs at day 7 of culture (original magnification, 10 $\times$ ). **F** BM EPCs at day 7 of culture were cultured in a transwell chamber for 24 h, fixed and then stained with crystal violet. Representative images (scale bars represent 200  $\mu$ m) of migrated cells on the bottom surface of the membrane (original magnification, 10 $\times$ ). **G** The number of migrated BM EPCs per field of view was compared (original magnification, 10 $\times$ ). Three power fields were randomly counted and averaged per sample. Statistical analyses were performed using the Mann–Whitney U test. Data are presented as the means  $\pm$  SEM (\**P*  $\leq$  0.05, \*\**P*  $\leq$  0.005, \*\*\**P*  $\leq$  0.001). AML Acute myeloid leukaemia, BM Bone marrow, BMMNCs Bone marrow mononuclear cells, EPCs Endothelial progenitor cells, Dil-Ac-LDL Dil-acetylated low-density lipoprotein, FITC-UEA I FITC-labelled Ulex Europaeus Agglutinin I, HD Healthy donor, H-MDS Higher-risk myelodysplastic syndromes, L-MDS Lower-risk myelodysplastic syndromes



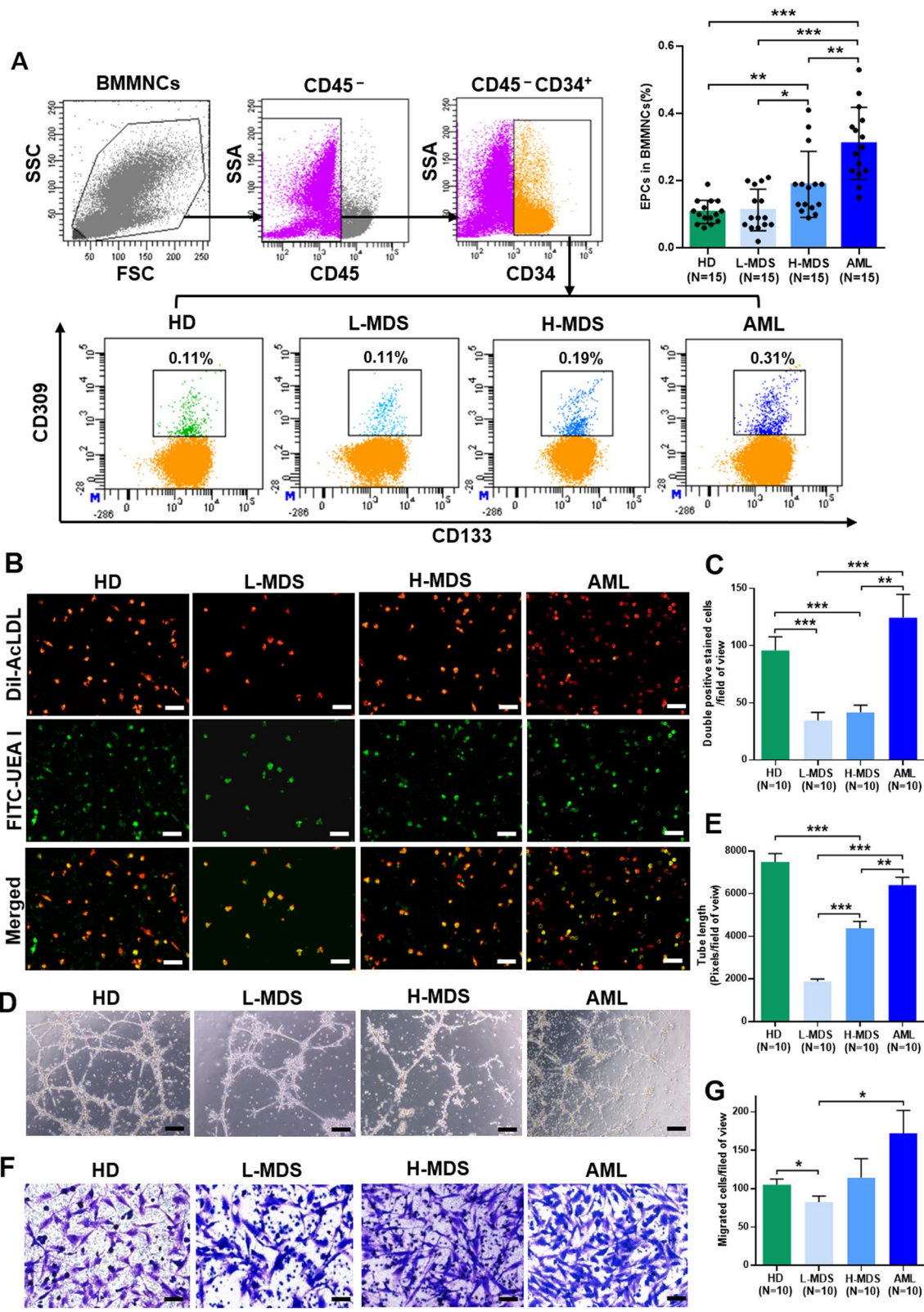


**Fig. 1** (See legend on previous page.)

## Results

### Increased number of BM EPCs in MDS patients

The representative BM EPC phenotype was characterized by CD34<sup>+</sup>CD309<sup>+</sup>CD133<sup>+</sup> by flow cytometry (Fig. 1A). The percentage of BM EPCs from higher-risk MDS patients (higher-risk MDS BM EPCs) (Fig. 1A,  $0.19\% \pm 0.03\%$  vs.  $0.11\% \pm 0.02\%$ ,  $P=0.03$ ) was significantly higher than BM EPCs from lower-risk MDS patients (lower-risk MDS BM EPCs), whereas the percentage of primary BM EPCs from AML patients (AML BM EPCs) was higher than higher-risk MDS BM EPCs (Fig. 1A,  $0.31\% \pm 0.03\%$  vs.  $0.19\% \pm 0.03\%$ ,  $P=0.002$ ).

After 7 days of cultivation, spindle-shaped and elongated BM adherent cells were further functionally characterized as EPCs, which were capable of DiI-AcLDL uptake and FITC-UEA I binding (the typical functional EPC markers) [28–30, 40, 41]. Moreover, EPC identity was confirmed by qRT-PCR for endothelial specific marker genes (VEGFR2, VE-cadherin and VWF) in Additional file 1: Fig. S1. The number of double-positive stained AML BM EPCs was significantly higher than higher-risk MDS BM EPCs (Fig. 1B and C,  $124.5 \pm 20.3$  vs.  $41.7 \pm 6.3$ ,  $P=0.003$ ). Together, increased numbers of BM EPCs were found in MDS patients, especially in more severe types of MDS.

### Decreased angiogenic potential but increased migration ability of BM EPCs in MDS patients

To evaluate the angiogenic potential and migration of BM EPCs from different types of MDS patients, tube formation and migration were analysed on day 7 of culture [28–30, 40]. Higher-risk MDS BM EPCs showed a significantly increased tube formation ability compared with lower-risk MDS BM EPCs (Fig. 1D and E,  $4375 \pm 321$  vs.  $1874.7 \pm 118.9$ ,  $P<0.0001$ ) and a markedly decreased tube formation ability compared with AML patients (Fig. 1D and E,  $4375 \pm 321$  vs.  $6403 \pm 370.4$ ,  $P=0.001$ ).

The AML BM EPCs on day 7 of culture showed increased migrated cells (Fig. 1F and G,  $172.4 \pm 29.8$  vs.  $82.6 \pm 7.9$ ,  $P=0.01$ ) compared with lower-risk MDS BM EPCs. These results demonstrated that the decreased angiogenic potential but increased migration capability in BM EPCs from MDS patients.

### RNA-seq indicates the progressive change and differences of haematopoiesis- and immune-related pathways and genes in MDS BM EPCs

To uncover the underlying mechanism of the variant dysfunctions in different types MDS BM EPCs, the lower-risk MDS BM EPCs ( $N=3$ ), higher-risk MDS BM EPCs ( $N=3$ ), AML patients BM EPCs ( $N=3$ ) and primary BM EPCs from HDs (HD BM EPCs) ( $N=3$ ) were analysed via RNA-seq (Fig. 2A). The results of PCA (Fig. 2B) and hierarchical clustering analysis (Fig. 2C) showed that the entire population was clearly separated into two distinct subpopulations, HD and disease BM EPCs. More importantly, the heatmap (Fig. 2C) of different groups showed the progressive change in the total RNA expression profile of HD BM EPCs, lower-risk MDS BM EPCs, and higher-risk MDS BM EPCs to AML BM EPCs. There were 886 different genes between lower-risk MDS and higher-risk MDS BM EPCs (Fig. 2D) and 825 different genes between higher-risk MDS and AML BM EPCs (Fig. 2E). KEGG pathway enrichment analysis of Organismal Systems class (Fig. 2F and G) indicated that haematopoiesis- and immune-related pathways were enriched in MDS BM EPCs. For example, haematopoietic cell lineage was enriched in both lower-risk MDS BM EPCs vs. higher-risk MDS BM EPCs and higher-risk MDS BM EPCs vs. AML BM EPCs. Th17 and Th2 cell differentiation and Th17 cell differentiation were enriched in higher-risk MDS BM EPCs vs. AML BM EPCs.

In addition, the previously reported haematopoiesis- and immunomodulation-related genes [51–56] in BM

(See figure on next page.)

**Fig. 2** Transcriptome heterogeneity of BM EPCs from MDS patients identified by bulk RNA-seq. **A** Schematic of the experiment. BM EPCs from 3 HDs and 3 L-MDS, 3 H-MDS, and 3 AML patients at 7 days of culture were collected, and bulk RNA-seq was performed. **B** PCA score plot of 12 libraries. **C** Heatmap and hierarchical clustering of RNA-seq data for the HD, L-MDS, H-MDS and AML groups using the Euclidean distance. Distributions and quantifications of genes in BM EPCs from **D** L-MDS versus H-MDS and **E** H-MDS versus AML. The x axis shows the log<sub>2</sub> of gene expression change, whereas the y axis shows the  $-\log_{10}$  of the  $P$  value. The KEGG pathway enrichment analyses of Organismal Systems class of the different genes between **F** L-MDS vs. H-MDS and **G** H-MDS vs. AML are shown. The x axis shows the rich factor. **H** Heatmap shows haematopoiesis- and immune-related gene expression in bulk RNA-seq data of 12 libraries. The relative mRNA levels of **I** *CXCL12*, *KITLG*, *NFKB1* genes and **J** *HAVCR2*, *CIITA*, *LGALS9* genes in HD, L-MDS, H-MDS and AML BM EPCs were determined using qRT-PCR. The relative mRNA analyses were using Wilcoxon matched-pairs signed rank test. Data are presented as the means  $\pm$  SEM ( $*P \leq 0.05$ ). *AML* Acute myeloid leukaemia, *BM* Bone marrow, *BMMNCs* Bone marrow mononuclear cells, *EPCs* Endothelial progenitor cells, *HD* Healthy donor, *H-MDS* Higher-risk myelodysplastic syndromes, *KEGG* Kyoto Encyclopedia of Genes and Genomes, *L-MDS* Lower-risk myelodysplastic syndromes, *PCA* Principal component analysis, *RNA-seq* RNA sequencing, *ROS* reactive oxygen species

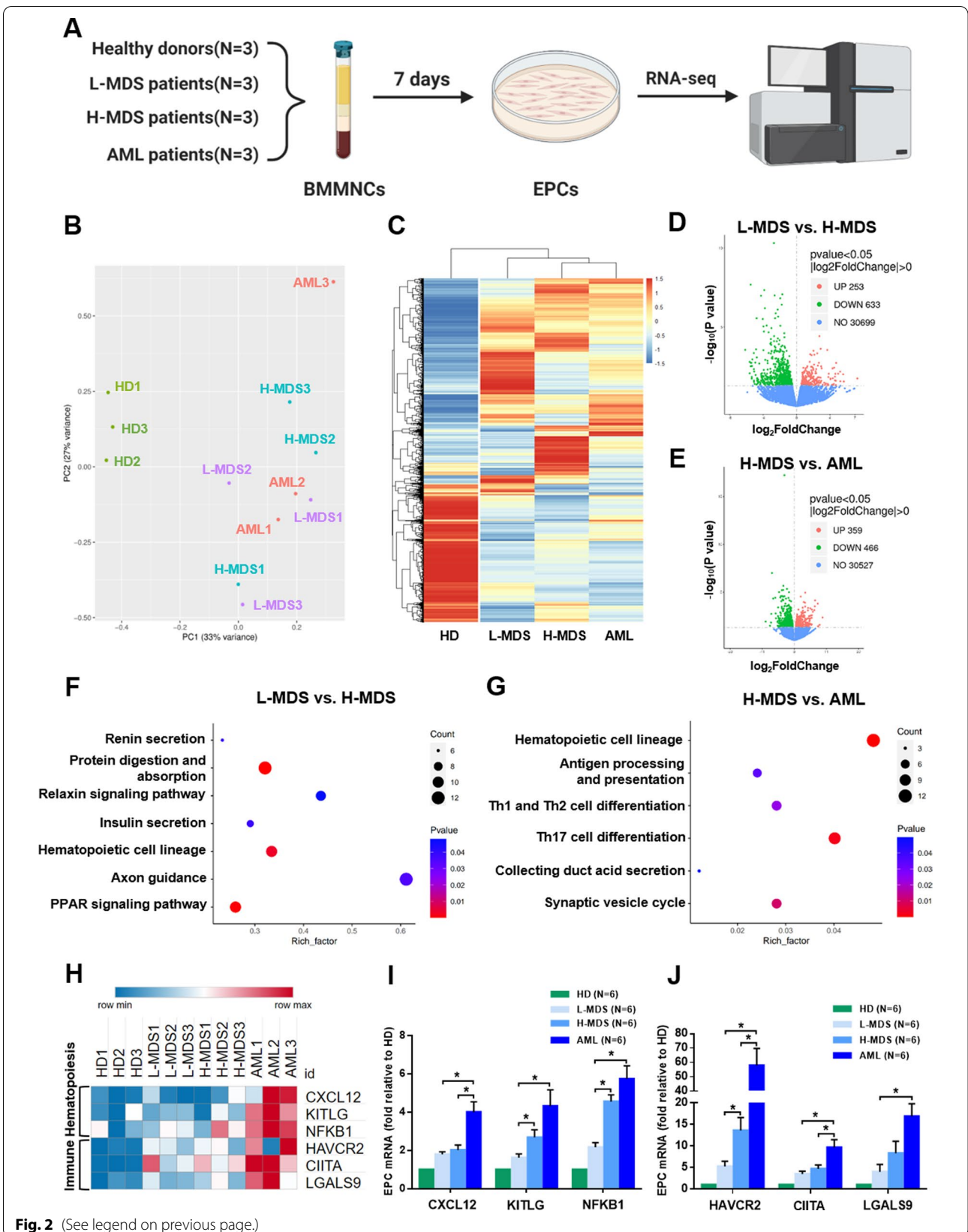


**Fig. 2** (See legend on previous page.)



EPCs were detected by RNA-seq (Fig. 2H) and verified by qRT-PCR. As shown in Fig. 2H–J, mRNA levels of haematopoiesis-related genes *CXCL12*, *KITLG*, *NFKB1* and immune-related genes *HAVCR2*, *LGALS9*, *CIITA* were increased in higher-risk MDS and AML BM EPCs compared with lower-risk MDS BM EPCs. These results suggested markedly enriched haematopoiesis- and immunomodulatory-related pathways and upregulation of related genes in higher-risk MDS BM EPCs. However, normal or malignant haematopoiesis-related genes could not be distinguished via RNA-seq analysis. Therefore, we further carried out in vitro experiments to analyse the haematopoiesis and immunomodulatory function of BM EPCs from MDS patients.

### Decreased ability of BM EPCs to support HSCs in higher-risk MDS patients

To investigate the effects of BM EPCs on HSCs in vitro, we sorted CD34<sup>+</sup> cells from BMMNCs of HDs with magnetic beads and cocultured them with BM EPCs. After 5 days, we analysed the apoptosis rates, intracellular ROS levels and CFU plating efficiencies of HSCs (Fig. 3A). Compared with the lower-risk MDS group, the higher-risk MDS group exhibited a marked increase in the apoptosis rates of HSCs after coculture (Fig. 3B and C, 21.09 ± 1.21% vs. 16.79 ± 0.97%, *P* = 0.01). The ROS level (Fig. 3D, 6039 ± 654.4 vs. 4308 ± 394.7, *P* = 0.03) of CD34<sup>+</sup> cells after coculture with AML BM EPCs was significantly higher than that of lower-risk MDS BM EPCs. HSCs cocultured with higher-risk MDS BM EPCs had lower CFU plating efficiencies than those cocultured with lower-risk MDS BM EPCs (Fig. 3E), as determined by CFU-E, BFU-E (12.9 ± 1.67 vs. 26.9 ± 3.62, *P* = 0.003), CFU-GM, and CFU-GEMM. The AML group had lower CFU-E, BFU-E, CFU-GM and CFU-GEMM plating efficiencies than the higher-risk MDS group. These data suggest that of MDS BM EPCs were less able to support HSCs in more severe type of MDS patients.

### BM EPCs induce T cell differentiation towards more immune-tolerant cells in higher-risk MDS patients

To further investigate the immunoregulatory effects of BM EPCs in vitro, we sorted CD3<sup>+</sup> cells from BMMNCs of HDs and cocultured them without or with HD BM EPCs, lower-risk MDS BM EPCs, higher-risk MDS BM EPCs and AML BM EPCs. After 3 days, we analysed differences in T cell subsets after coculture or not (control of T cell alone cultures) (Fig. 4A). The subtypes of Th1 cells, Th2 cells, Th17 cells and Tregs were characterized by positive expression of CD4<sup>+</sup>IFN-γ<sup>+</sup>, CD4<sup>+</sup>IL-4<sup>+</sup>, CD4<sup>+</sup>IL-17<sup>+</sup> and CD4<sup>+</sup>CD25<sup>+</sup>Foxp3<sup>+</sup>, respectively (Fig. 4B). There was a markedly lower percentage of Th1 cells in the AML group than in the higher-risk MDS group (Fig. 4C, 4.86% ± 0.54% vs. 8.07% ± 0.51%, *P* = 0.004) and in the higher-risk MDS group than in the lower-risk MDS group (Fig. 4C, 8.07% ± 0.51% vs. 9.95% ± 0.6%, *P* = 0.04). A significantly lower percentage of Th17 cells was observed in the higher-risk MDS group than in the lower-risk MDS group (Fig. 4D, 6.54% ± 0.43% vs. 9.35% ± 0.92%, *P* = 0.004) and in the AML group than in the higher-risk MDS group (Fig. 4D, 4.48% ± 0.58% vs. 6.54% ± 0.43%, *P* = 0.04). However, higher percentages of Th2 cells (Fig. 4E, 8.77% ± 1.0% vs. 5.67% ± 0.31%, *P* = 0.02) in the higher-risk MDS group than in the lower-risk MDS group. In addition, higher percentages of Tregs (Fig. 4F, 4.74% ± 0.59% vs. 3.14% ± 0.31%, *P* = 0.01) were observed in the AML group than in the higher-risk MDS group. As a result, the ratio of Th1/Th2 cells was markedly lower in the higher-risk MDS group than in the lower-risk MDS group (Fig. 4G, 1.0 ± 0.1 vs. 1.81 ± 0.17, *P* = 0.004), whereas that was significantly lower in the AML group than in the higher-risk MDS group (Fig. 4G, 0.51 ± 0.06 vs. 1.0 ± 0.1, *P* = 0.02). These data showed that lower-risk MDS BM EPCs regulated T cell differentiation into Th17 cells, whereas higher-risk MDS and AML BM EPCs regulated T cell differentiation into Th2 cells and Tregs. Our data suggested that BM EPCs might be

(See figure on next page.)

**Fig. 3** Supporting abilities of BM EPCs from MDS patients to HSCs. **A** Schematic diagram of the study design for the BM EPC coculture process with HSCs. After 5 days of coculture, the apoptosis ratio and the quantification of the level of intracellular ROS and CFU efficiencies of HSCs were detected. Representative images (**B**) and quantification (**C**) of the apoptosis ratio of HSCs after coculture with BM EPCs are shown. Quantification (**D**, left) and representative images (**D**, right) of the ROS levels (MFI) of HSCs after coculture are shown. **E** The CFU plating efficiencies of HSCs, including CFU-E, BFU-E, CFU-GM and CFU-GEMM, after coculture with BM EPCs from HDs, L-MDS, H-MDS and AML patients. Statistical analyses were performed using the Mann–Whitney U test. Data are presented as the means ± SEM (\**P* ≤ 0.05, \*\* *P* ≤ 0.005, \*\*\* *P* ≤ 0.001). *AML* Acute myeloid leukaemia, *BFU-E* Burst-forming unit erythroid, *BM* Bone marrow, *BMMNCs* Bone marrow mononuclear cells, *CFU* Colony-forming unit, *CFU-E* Colony-forming unit erythroid, *CFU-GM* Colony-forming unit-granulocyte/macrophages, *CFU-GEMM* Colony-forming unit-granulocyte, erythroid, macrophage and megakaryocyte, *EPCs* Endothelial progenitor cells, *HD* Healthy donor, *HSC* haematopoietic stem cells, *H-MDS* Higher-risk myelodysplastic syndromes, *L-MDS* Lower-risk myelodysplastic syndromes



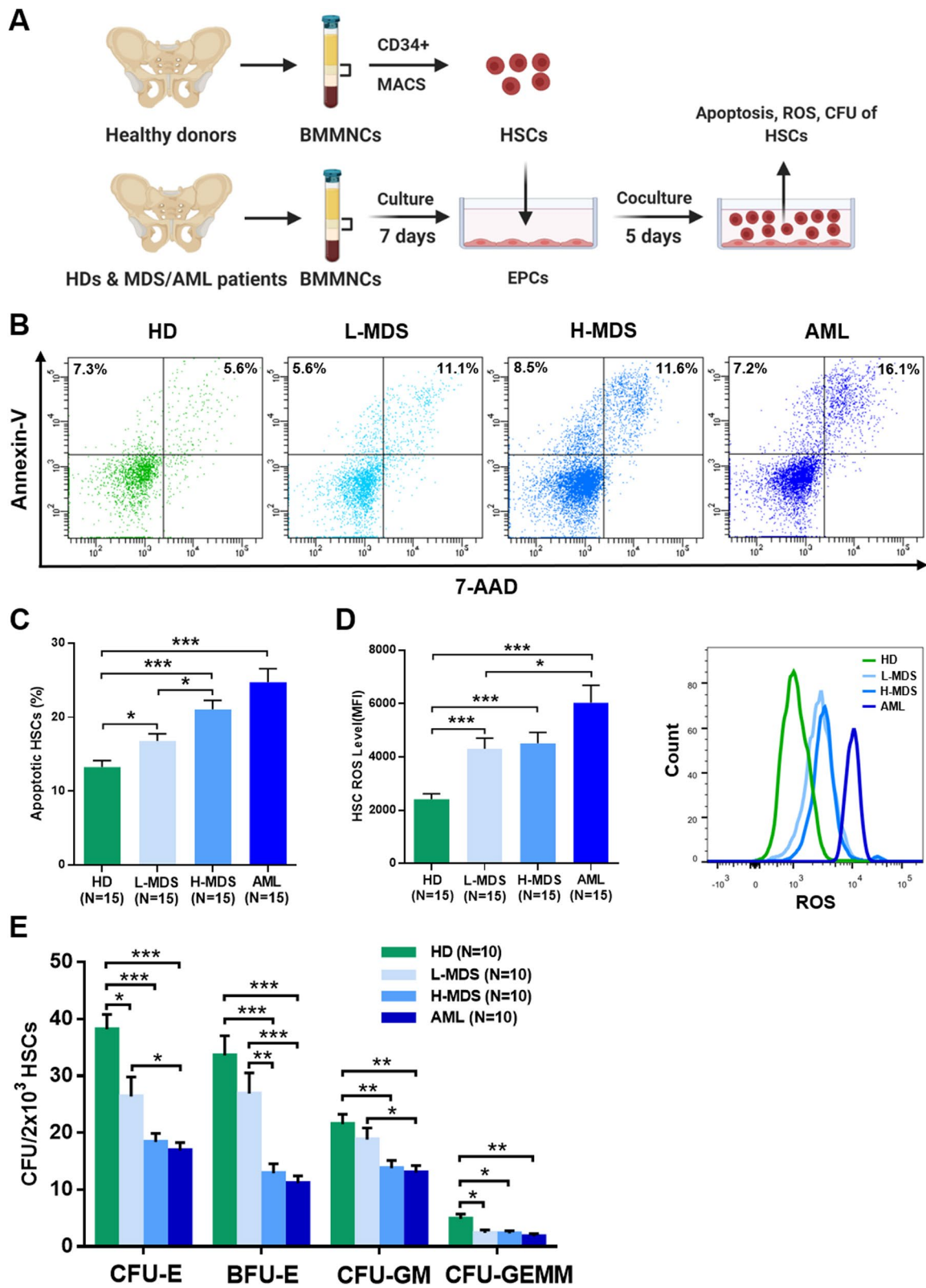


**Fig. 3** (See legend on previous page.)

inclined to induce T cell differentiation towards more immune-tolerant cells in higher-risk MDS patients.

#### Increased ability of BM EPCs to support leukaemia cells in higher-risk MDS patients

To investigate the effect of BM EPCs on leukaemia cells in vitro, we assessed the proliferation, apoptosis and CFU-L plating efficiency of HL-60 cells after coculture with BM EPCs (Fig. 5A). In addition, the relative mRNA expression levels of apoptosis- and cell cycle-related genes were detected in HL-60 cells after coculture. The EdU -positive rate of HL-60 cells was significantly higher in the higher-risk MDS group than in the lower-risk MDS group (Fig. 5B and C,  $45.79\% \pm 1.12\%$  vs.  $36.52\% \pm 2.20\%$ ,  $P=0.003$ ). More importantly, CFU-L plating efficiencies were markedly increased in AML group compared with higher-risk MDS group (Fig. 5D and E,  $374.1 \pm 37.2$  vs.  $257.6 \pm 33.2$ ,  $P=0.04$ ). However, the apoptotic rate of HL-60 cells was notably decreased in the AML group compared with the lower-risk MDS group (Fig. 5F,  $2.6\% \pm 0.52\%$  vs.  $4.38\% \pm 0.46\%$ ,  $P=0.01$ ). The *CASP2*, *CASP3*, *BAX*, *TP53* and *CDKN1A* mRNA levels in HL-60 cells were downregulated, whereas the *CCNE1* and *MCL1* mRNA levels were upregulated in the higher-risk MDS and AML groups than the lower-risk MDS group (Fig. 5G). These data suggest that BM EPCs may become more supportive of leukaemia cells in higher-risk MDS patients.

#### The levels of ROS and the apoptosis ratio were increased in BM EPCs from higher-risk MDS patients

To further explore the internal changes in dysfunctional EPCs and identify underlying therapeutic targets, we investigated damage related pathways from the RNA-seq data. GSEA highlighted abnormalities of mitochondrial signaling pathway (Fig. 6A, B), so we verified them by detecting ROS levels of precultivated and cultivated BM EPCs. The ROS level of precultivated AML BM EPCs was significantly higher than that in higher-risk MDS BM EPCs (Fig. 6C,  $5369 \pm 426.0$  vs.  $3039 \pm 335.3$ ,  $P=0.0002$ ).

The ROS level in the cultivated AML BM EPCs was higher than that in the cultivated higher-risk MDS BM EPCs, whereas the ROS level of the cultivated higher-risk MDS BM EPCs was higher than that in the lower-risk MDS BM EPCs (Fig. 6D, E). Moreover, the pathway of apoptotic nuclear changes was identified in GSEA (Fig. 6F). The apoptosis rate (Fig. 6G,  $43.79\% \pm 2.77\%$  vs.  $20.63\% \pm 3.01\%$ ,  $P<0.0001$ ) was significantly higher in AML BM EPCs than in lower-risk MDS EPCs. The relative mRNA expression levels of apoptosis-related genes in BM EPCs were further analysed by qRT-PCR. The *CASP2* mRNA level was significantly upregulated in AML BM EPCs (Fig. 6H,  $6.43 \pm 0.89$ -fold vs.  $2.28 \pm 0.56$ -fold,  $P=0.03$ ) compared to higher-risk MDS BM EPCs. The *CASP3* (Fig. 6H,  $2.09 \pm 0.26$ -fold vs.  $0.88 \pm 0.3$ -fold,  $P=0.03$ ) and *BAX* (Fig. 6H,  $2.0 \pm 0.35$ -fold vs.  $1.08 \pm 0.14$ -fold,  $P=0.03$ ) mRNA levels were significantly upregulated in higher-risk MDS BM EPCs compared to lower-risk MDS BM EPCs. Together, elevated levels of ROS and apoptosis of BM EPCs were found in MDS patients, especially in higher-risk MDS patients, which may be the underlying repair targets for MDS patients (Fig. 7).

#### Discussion

The current study firstly demonstrated increased but dysfunctional BM EPCs in patients with MDS. The abilities of BM EPCs from higher-risk MDS patients to support HSCs decreased, whereas those from higher-risk MDS patients to support leukaemia cells increased. Furthermore, BM EPCs might be inclined to induce T cell differentiation towards more immune-tolerant cells in more severe type of MDS patients. In addition, excessive production of ROS and apoptotic pathway activation may be the underlying mechanisms of dysfunctional BM EPCs. Our data indicate that repair of dysfunctional BM EPCs may be a potential therapeutic approach for MDS patients.

Increased BM angiogenesis has been reported in MDS patients [32, 57–59]. Immunohistochemical studies have

(See figure on next page.)

**Fig. 4** Regulatory abilities of BM EPCs from MDS patients to differentiate T cells. **A** Schematic diagram of the study design for BM EPC coculture processes with T cells. After 3 days of coculture, the differentiation of T cells was analysed by flow cytometry. **B** The subtypes of Th1 cells, Th2 cells, Th17 cells and Tregs were characterized by positive expression of  $CD4^+IFN-\gamma^+$ ,  $CD4^+IL-4^+$ ,  $CD4^+IL-17^+$  and  $CD4^+CD25^+Foxp3^+$ , respectively. The percentage of **C** Th1 cells, **D** Th17 cells, **E** Th2 cells, **F** Tregs and **G** the ratio of Th1/Th2 cells after coculture without (Control) or with HD-derived, L-MDS, H-MDS, AML patient-derived BM EPCs for 3 days. The paired analyses were using Wilcoxon matched-pairs signed rank test. Data are presented as the means  $\pm$  SEM ( $*P \leq 0.05$ ,  $**P \leq 0.005$ ). *AML* Acute myeloid leukaemia, *BM* Bone marrow, *BMMNCs* Bone marrow mononuclear cells, *EPCs* Endothelial progenitor cells, *HD* Healthy donor, *H-MDS* Higher-risk myelodysplastic syndromes, *L-MDS* Lower-risk myelodysplastic syndromes, *Th* T helper, *Tregs* Regulatory T cells, *ROS* reactive oxygen species

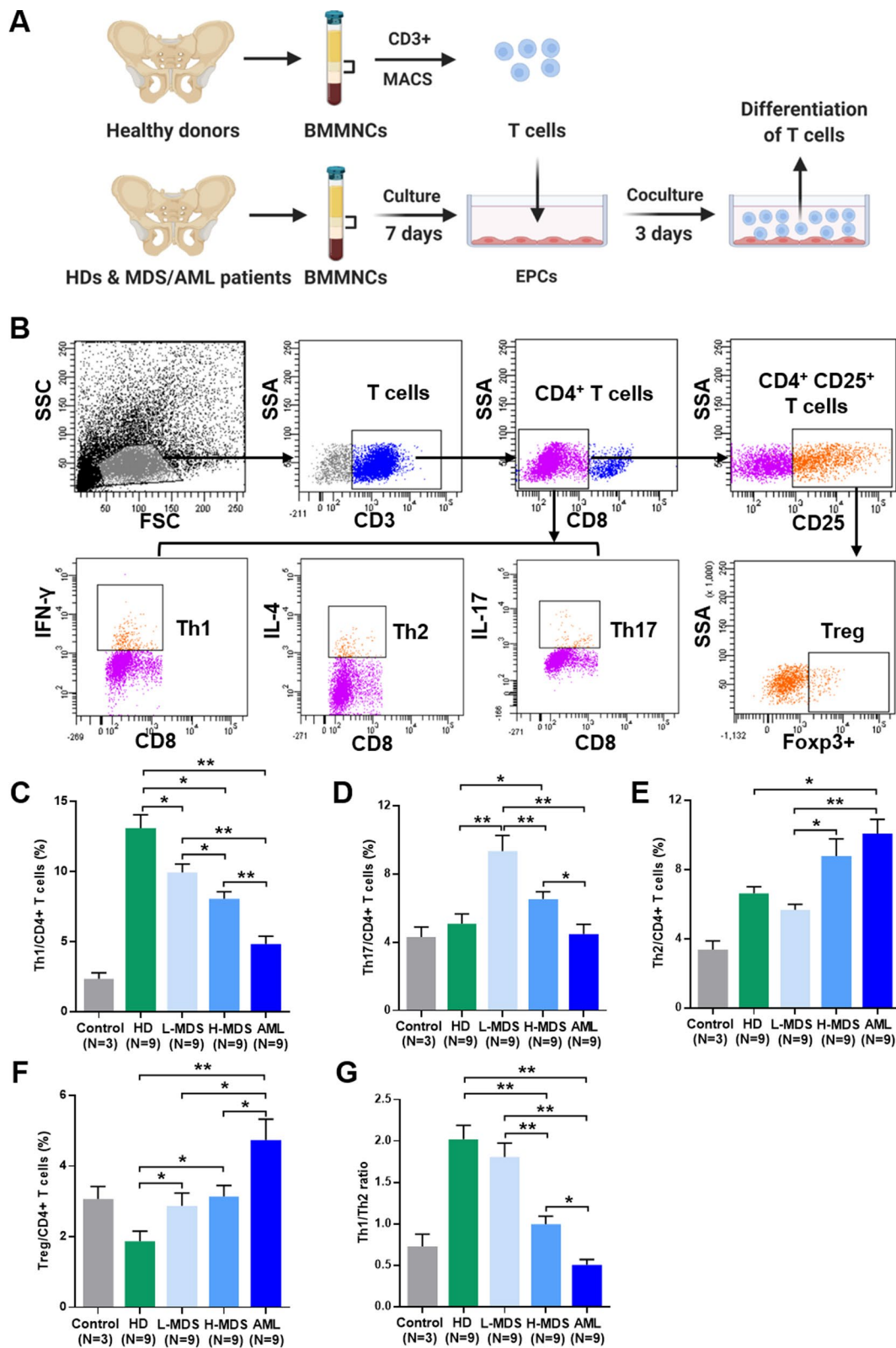


**Fig. 4** (See legend on previous page.)

demonstrated an increased microvessel density (MVD) in the biopsies of MDS patients [58–60]. The results concerning the correlation between BM MVD and classification are controversial. Some studies reported a higher MVD preferentially among higher-risk MDS patients [58, 61], while other studies failed to find such a correlation [60]. Other studies regarding circulating endothelial cells and peripheral EPCs are consistently increased in MDS patients compared with normal controls [32, 57]. In summary, the number of BM EPCs in MDS patients and their correlation with the different risk degrees are not clear. More importantly, the functions of BM EPCs in patients with different risk groups of MDS are largely unknown. Our study firstly demonstrated increased BM EPCs with dysfunctions in MDS patients, especially more severe dysfunctions of BM EPCs in patients with higher-risk MDS. We speculated that the increased and dysfunctional EPCs in MDS patients were responsible for more nutrient and metabolite turnover, and may secrete more cytokines to better support malignant hematopoiesis. Based on our previous work and the current study, the impairment of EPCs was associated with elevated intracellular ROS levels and an elevated apoptosis ratio in MDS patients [28, 29, 39, 62]. Therefore, it is worth investigating the efficacy of therapeutic strategies, such as *N*-acetyl-L-cysteine (a reactive oxygen species scavenger) [28, 29, 62, 63] or inhibitor of EPC-targeted apoptosis pathways, to improve the prognosis of MDS patients by enhancing BM EPCs in the future.

A great deal of researches have certified the critical role of EPCs in regulating haematopoiesis [24, 26, 27], whereas Hatfield et al. found that EPCs supported leukaemia cells by directly enhancing the proliferation and inhibiting apoptosis of AML blasts [45]. However, it is unclear whether the abilities of BM EPCs from MDS patients to support HSCs or leukaemia cells are the same

or different. Surprisingly, we found antipodal results for normal HSCs and leukaemia cells. The CFU plating efficiency of HSCs declined with disease progression, which suggested BM EPCs from patients with MDS or AML could not support normal differentiation of HSCs. On the contrary, the CFU-L plating efficiency increased, which implied the possible role of BM EPCs as an oncogenic driver or facilitator of MDS. On the other hand, the progression of MDS is also facilitated by immune deregulation [1]. However, the correlation between BM EPCs and immune deregulation in MDS is largely unknown. Consistent with previous clinical reports of T cell subtypes in MDS patients [21, 22], our data demonstrated that BM EPCs from lower-risk MDS patients regulate T cell differentiation into inflammatory Th17 cells but BM EPCs from higher-risk MDS patients regulate T cells into more immune tolerant cells.

We are aware that the underlying mechanism on how BM EPCs regulate T cells and the precise T cell subset need to be further explored in the future. However, our data indicated that the dysregulated immunomodulatory function of EPCs may also contribute to ineffective haematopoiesis and evasion from antitumoural immunity in MDS. Therefore, in conjunction with existing therapies, improvement of BM EPCs may be a potential therapeutic strategy for patients with MDS.

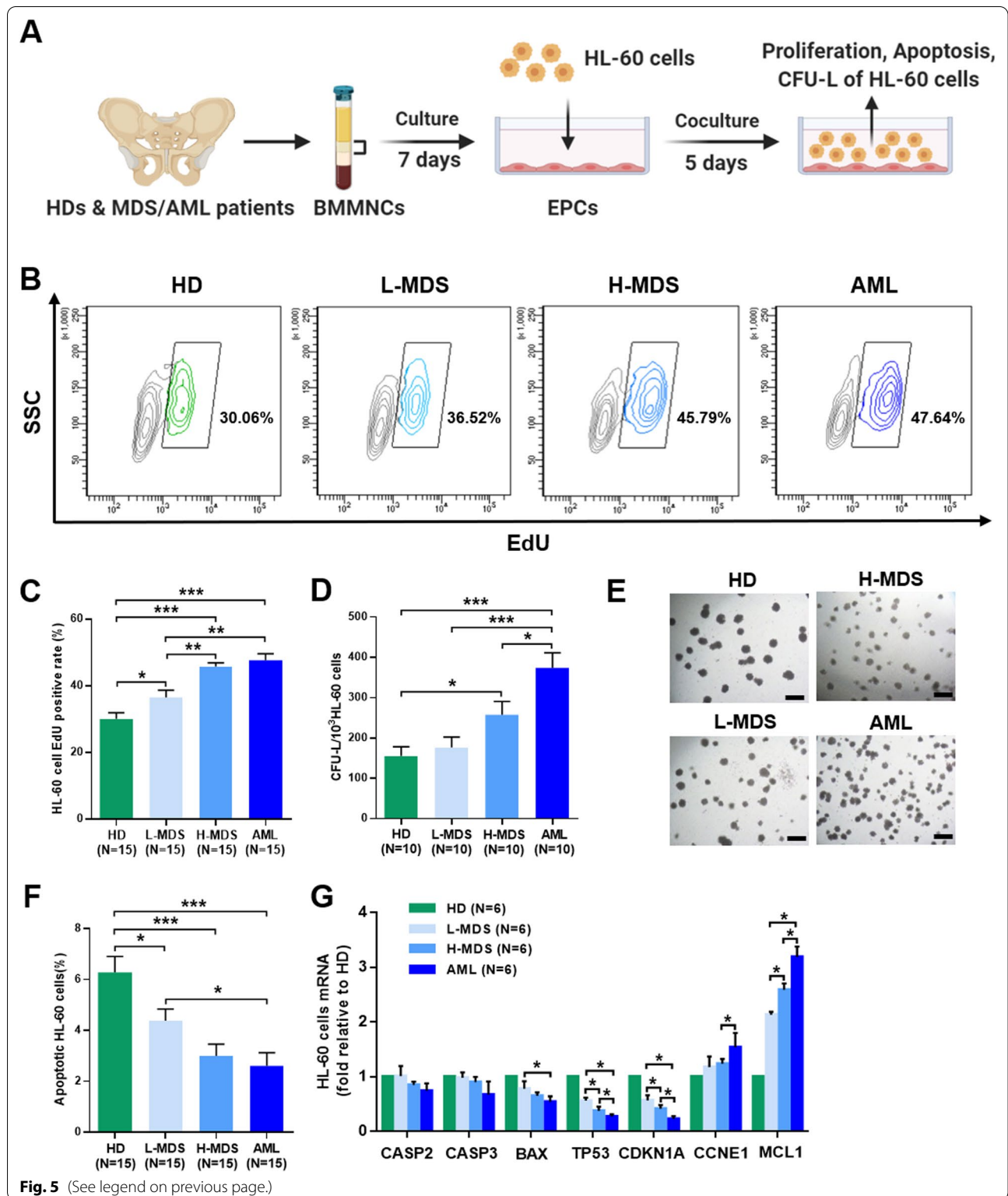
## Conclusions

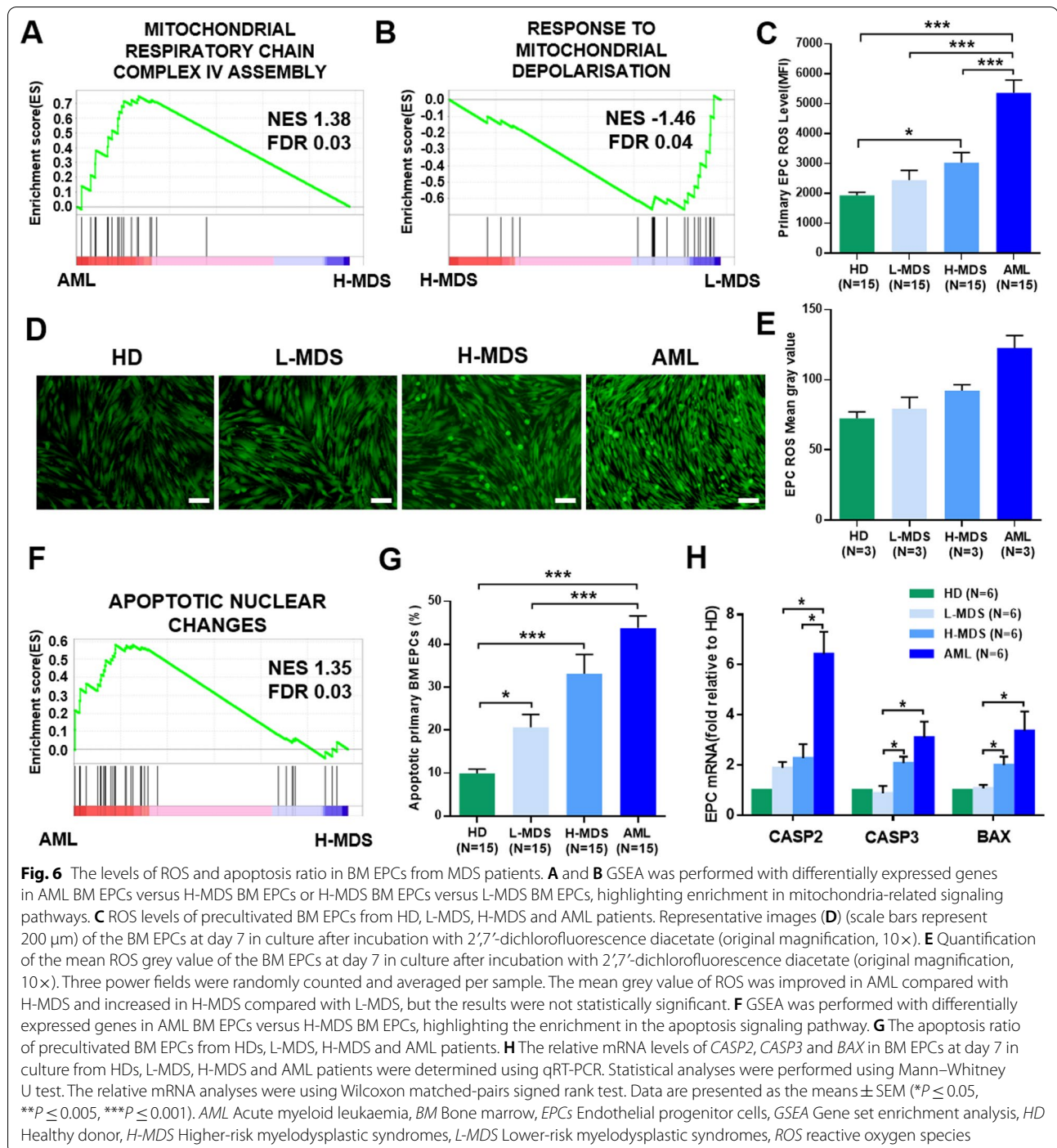
In summary, the current study demonstrated that dysfunctional BM EPCs were involved in MDS patients. Changes in the BM microenvironment may be a primary driver of human haematological malignancies, as has been suggested by animal models [64, 65]. Although further validation is required, our findings indicate that improving BM EPCs may represent a potential therapeutic approach for MDS patients.

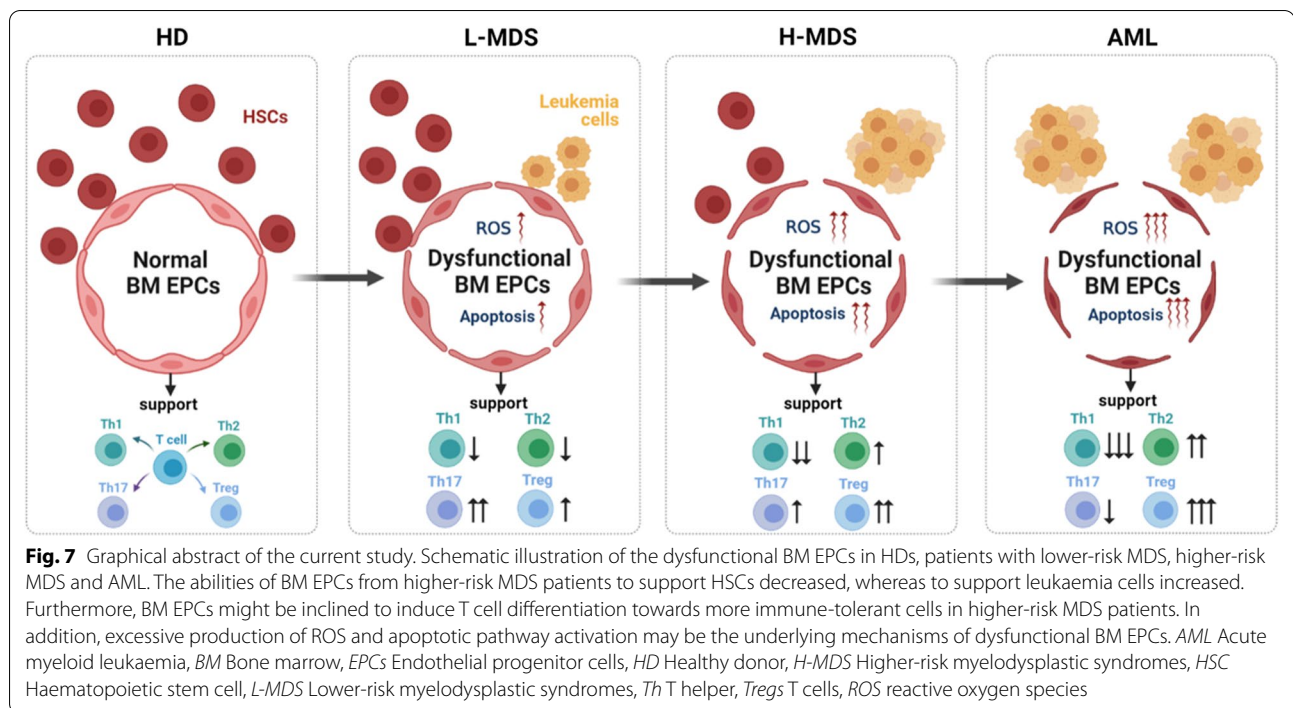
(See figure on next page.)

**Fig. 5** Supporting abilities of BM EPCs from MDS patients to leukaemia cells. **A** Schematic diagram of the study design for BM EPC coculture processes with HL-60 cells. After 5 days of coculture, the EdU-positive rates, apoptosis ratio and CFU-L efficiencies of HL-60 cells were detected. Representative images (**B**) and quantification of the EdU-positive rates (**C**) of HL-60 cells after coculture with BM EPCs are shown. Quantification (**D**) of the CFU-L plating efficiencies and representative images (scale bars represent 500  $\mu$ m) (**E**) of CFU-L after coculture with BM EPCs are shown (original magnification, 4 $\times$ ). Three power fields were randomly counted and averaged per sample. **F** Quantification of the apoptosis ratio of HL-60 cells after coculture. **G** The relative mRNA levels of *CASP2*, *CASP3*, *BAX*, *TP53*, *CDKN1A*, *CCNE1* and *MCL1* in HL-60 cells after coculture with BM EPCs were determined by qRT-PCR. Statistical analyses were performed using the Mann–Whitney U test. The relative mRNA analyses were using Wilcoxon matched-pairs signed rank test. Data are presented as the means  $\pm$  SEM (\* $P \leq 0.05$ , \*\* $P \leq 0.005$ , \*\*\* $P \leq 0.001$ ). *AML* Acute myeloid leukaemia, *BM* Bone marrow, *BMMNCs* Bone marrow mononuclear cells, *CFU-L* Leukaemia colony-forming unit, *EdU* 5-ethynyl-20 deoxyuridine, *EPCs* Endothelial progenitor cells, *HD* Healthy donor, *H-MDS* Higher-risk myelodysplastic syndromes, *L-MDS* Lower-risk myelodysplastic syndromes









### Abbreviations

Allo-HSCT: Allogeneic haematopoietic stem cell transplantation; AML: Acute myeloid leukaemia; BFU-E: Burst-forming unit erythroid; BM: Bone marrow; BMMNCs: Bone marrow mononuclear cells; CFU: Colony-forming unit; CFU-E: Colony-forming unit erythroid; CFU-GM: Colony-forming unit-granulocyte/macrophages; CFU-GEMM: Colony-forming unit-granulocyte, erythroid, macrophage and megakaryocyte; CFU-L: Leukaemia colony-forming unit; DEG: Differential gene expression; Dil-Ac-LDL: Dil-acetylated low-density lipoprotein; Edu: 5-Ethynyl-20-deoxyuridine; EPCs: Endothelial progenitor cells; FITC-UEAI: FITC-labelled Ulex Europaeus Agglutinin I; GSEA: Gene set enrichment analysis; HDs: Healthy donors; HSC: Haematopoietic stem cell; IPSS-R: Revised International Prognostic Scoring System; KEGG: Kyoto Encyclopedia of Genes and Genomes; MDS: Myelodysplastic syndromes; PCA: Principal component analysis; qRT-PCR: Real-time quantitative polymerase chain reaction; RNA-seq: RNA sequencing; ROS: Reactive oxygen species; Th: T helper; Tregs: T cells; VEGFR2: Vascular endothelial growth factor receptor 2; 7-AAD: 7-Amino-actinomycin D.

### Supplementary Information

The online version contains supplementary material available at <https://doi.org/10.1186/s12967-022-03354-2>.

**Additional file 1: Figure S1.** Validation of EPC identity. **Table S1.** Clinical characteristics of MDS patients. **Table S2.** Antibody information. **Table S3.** Top 20 up and down regulated genes in higher-risk MDS BM EPCs than lower-risk MDS BM EPCs. **Table S4.** Top 20 up and down regulated genes in AML BM EPCs than higher-risk MDS BM EPCs. **Table S5.** The primer sequences of genes used for qRT-PCR.

### Acknowledgements

The authors thank all of the core facilities at Peking University Institute of Hematology for patient care and sample collection. American Journal Experts ([www.journalexperts.com](http://www.journalexperts.com)) provided editorial assistance to the authors during the preparation of the manuscript. The model in Figures was created with [www.biorender.com](http://www.biorender.com).

### Authors' contributions

YK designed the study. YK and XJH supervised the manuscript preparation. TX, and YK performed the research and wrote the manuscript. All other authors participated in the collection of patient data. All authors read and approved the final manuscript.

### Funding

This work was supported by National Key R&D Program of China (2021YFA1100904 & 2019YFC0840606), National Natural Science Foundation of China (82070188 & 81870139 & 81930004), and the Foundation for Innovative Research Groups of the National Natural Science Foundation of China (81621001).

### Availability of data and materials

All data needed to evaluate the conclusions in the paper are present in the paper and/or the Additional file. The accession number of whole transcriptome RNA-seq data is GSE197907.

### Declarations

#### Ethics approval and consent to participate

The study was approved by the Ethics Committee of Peking University People's Hospital, and written informed consent was obtained from all subjects in compliance with the Declaration of Helsinki.

#### Consent for publication

Not applicable.

#### Competing interests

The authors declare that they have no competing interests.

#### Author details

<sup>1</sup>Peking University People's Hospital, Peking University Institute of Hematology, National Clinical Research Center for Hematologic Disease, Beijing Key Laboratory of Hematopoietic Stem Cell Transplantation, Collaborative Innovation Center of Hematology, Peking University, Beijing, China. <sup>2</sup>Peking-Tsinghua

Center for Life Sciences, Academy for Advanced Interdisciplinary Studies, Peking University, Beijing, China. <sup>3</sup>Key Laboratory of Pediatric Hematology and Oncology Ministry of Health and Pediatric Translational Medicine Institute, Shanghai Children's Medical Center, Shanghai Collaborative Innovation Center for Translational Medicine and Department of Pharmacology and Chemical Biology, Shanghai Jiao Tong University School of Medicine, Shanghai, China.

Received: 3 February 2022 Accepted: 17 March 2022

Published online: 29 March 2022

## References

- Ades L, Itzykson R, Fenaux P. Myelodysplastic syndromes. *Lancet*. 2014;383(9936):2239–52.
- Cazzola M. Myelodysplastic syndromes. *N Engl J Med*. 2020;383(14):1358–74.
- Tefferi A, Vardiman JW. Myelodysplastic syndromes. *N Engl J Med*. 2009;361(19):1872–85.
- Yang L, Qian Y, Eksioglu E, Epling-Burnette PK, Wei S. The inflammatory microenvironment in MDS. *Cell Mol Life Sci*. 2015;72(10):1959–66.
- Bulycheva E, Rauner M, Medyouf H, Theurl I, Bornhauser M, Hofbauer LC, et al. Myelodysplasia is in the niche: novel concepts and emerging therapies. *Leukemia*. 2015;29(2):259–68.
- Malcovati L, Hellstrom-Lindberg E, Bowen D, Ades L, Cermak J, Del Canizo C, et al. Diagnosis and treatment of primary myelodysplastic syndromes in adults: recommendations from the European LeukemiaNet. *Blood*. 2013;122(17):2943–64.
- Stahl M, DeVeaux M, de Witte T, Neukirchen J, Sekeres MA, Brunner AM, et al. The use of immunosuppressive therapy in MDS: clinical outcomes and their predictors in a large international patient cohort. *Blood Adv*. 2018;2(14):1765–72.
- Guo H, Chang YJ, Hong Y, Xu LP, Wang Y, Zhang XH, et al. Dynamic immune profiling identifies the stronger graft-versus-leukemia (GVL) effects with haploidentical allografts compared to HLA-matched stem cell transplantation. *Cell Mol Immunol*. 2021;18(5):1172–85.
- Zhang XH, Chen J, Han MZ, Huang H, Jiang EL, Jiang M, et al. The consensus from The Chinese Society of Hematology on indications, conditioning regimens and donor selection for allogeneic hematopoietic stem cell transplantation: 2021 update. *J Hematol Oncol*. 2021;14(1):145.
- Cutler CS, Lee SJ, Greenberg P, Deeg HJ, Perez WS, Anasetti C, et al. A decision analysis of allogeneic bone marrow transplantation for the myelodysplastic syndromes: delayed transplantation for low-risk myelodysplasia is associated with improved outcome. *Blood*. 2004;104(2):579–85.
- Sorror ML, Sandmaier BM, Storer BE, Maris MB, Baron F, Maloney DG, et al. Comorbidity and disease status based risk stratification of outcomes among patients with acute myeloid leukemia or myelodysplasia receiving allogeneic hematopoietic cell transplantation. *J Clin Oncol*. 2007;25(27):4246–54.
- Della Porta MG, Alessandrino EP, Bacigalupo A, van Lint MT, Malcovati L, Pascutto C, et al. Predictive factors for the outcome of allogeneic transplantation in patients with MDS stratified according to the revised IPSS-R. *Blood*. 2014;123(15):2333–42.
- Lindsley RC, Saber W, Mar BG, Redd R, Wang T, Haagenson MD, et al. Prognostic mutations in myelodysplastic syndrome after stem-cell transplantation. *N Engl J Med*. 2017;376(6):536–47.
- Woll PS, Kjallquist U, Chowdhury O, Doolittle H, Wedge DC, Thongjuea S, et al. Myelodysplastic syndromes are propagated by rare and distinct human cancer stem cells in vivo. *Cancer Cell*. 2014;25(6):794–808.
- Cazzola M, Della Porta MG, Malcovati L. The genetic basis of myelodysplasia and its clinical relevance. *Blood*. 2013;122(25):4021–34.
- Walter MJ, Shen D, Ding L, Shao J, Koboldt DC, Chen K, et al. Clonal architecture of secondary acute myeloid leukemia. *N Engl J Med*. 2012;366(12):1090–8.
- Kennedy AL, Shimamura A. Genetic predisposition to MDS: clinical features and clonal evolution. *Blood*. 2019;133(10):1071–85.
- Raza A, Galili N. The genetic basis of phenotypic heterogeneity in myelodysplastic syndromes. *Nat Rev Cancer*. 2012;12(12):849–59.
- Winter S, Shoaie S, Kordasti S, Platzbecker U. Integrating the “immunome” in the stratification of myelodysplastic syndromes and future clinical trial design. *J Clin Oncol*. 2020;38(15):1723–35.
- Zou JX, Rollison DE, Boulware D, Chen DT, Sloand EM, Pflannes LV, et al. Altered naive and memory CD4+ T-cell homeostasis and immunosenescence characterize younger patients with myelodysplastic syndrome. *Leukemia*. 2009;23(7):1288–96.
- Kordasti SY, Afzali B, Lim Z, Ingram W, Hayden J, Barber L, et al. IL-17-producing CD4(+) T cells, pro-inflammatory cytokines and apoptosis are increased in low risk myelodysplastic syndrome. *Br J Haematol*. 2009;145(1):64–72.
- Kordasti SY, Ingram W, Hayden J, Darling D, Barber L, Afzali B, et al. CD4+CD25high Foxp3+ regulatory T cells in myelodysplastic syndrome (MDS). *Blood*. 2007;110(3):847–50.
- Duarte D, Hawkins ED, Lo CC. The interplay of leukemia cells and the bone marrow microenvironment. *Blood*. 2018;131(14):1507–11.
- Mendez-Ferrer S, Bonnet D, Steensma DP, Hasserjian RP, Ghibrial IM, Gribben JG, et al. Bone marrow niches in hematological malignancies. *Nat Rev Cancer*. 2020;20(5):285–98.
- Zambetti NA, Ping Z, Chen S, Kenswil KJG, Mylona MA, Sanders MA, et al. Mesenchymal inflammation drives genotoxic stress in hematopoietic stem cells and predicts disease evolution in human pre-leukemia. *Cell Stem Cell*. 2016;19(5):613–27.
- Morrison SJ, Scadden DT. The bone marrow niche for hematopoietic stem cells. *Nature*. 2014;505(7483):327–34.
- Ding L, Saunders TL, Enikolopov G, Morrison SJ. Endothelial and perivascular cells maintain hematopoietic stem cells. *Nature*. 2012;481(7382):457–62.
- Shi MM, Kong Y, Song Y, Sun YQ, Wang Y, Zhang XH, et al. Atorvastatin enhances endothelial cell function in posttransplant poor graft function. *Blood*. 2016;128(25):2988–99.
- Kong Y, Shi MM, Zhang YY, Cao XN, Wang Y, Zhang XH, et al. N-acetyl-L-cysteine improves bone marrow endothelial progenitor cells in prolonged isolated thrombocytopenia patients post allogeneic hematopoietic stem cell transplantation. *Am J Hematol*. 2018;93(7):931–42.
- Lyu ZS, Cao XN, Wen Q, Mo XD, Zhao HY, Chen YH, et al. Autophagy in endothelial cells regulates their hematopoiesis-supporting ability. *EBioMedicine*. 2020;53:102677.
- Balderman SR, Li AJ, Hoffman CM, Frisch BJ, Goodman AN, LaMere MW, et al. Targeting of the bone marrow microenvironment improves outcome in a murine model of myelodysplastic syndrome. *Blood*. 2016;127(5):616–25.
- Teofili L, Martini M, Nuzzolo ER, Capodimonti S, Iachinoto MG, Cocomazzi A, et al. Endothelial progenitor cell dysfunction in myelodysplastic syndromes: possible contribution of a defective vascular niche to myelodysplasia. *Neoplasia*. 2015;17(5):401–9.
- Cogle CR, Goldman DC, Madlambayan GJ, Leon RP, Masri AA, Clark HA, et al. Functional integration of acute myeloid leukemia into the vascular niche. *Leukemia*. 2014;28(10):1978–87.
- Lim WC, Olding M, Healy E, Millar TM. Human endothelial cells modulate CD4(+) T cell populations and enhance regulatory T cell suppressive capacity. *Front Immunol*. 2018;9:565.
- Al-Soudi A, Kaajj MH, Tas SW. Endothelial cells: from innocent bystanders to active participants in immune responses. *Autoimmun Rev*. 2017;16(9):951–62.
- Bedke T, Pretsch L, Karakhanova S, Enk AH, Mahnke K. Endothelial cells augment the suppressive function of CD4+ CD25+ Foxp3+ regulatory T cells: involvement of programmed death-1 and IL-10. *J Immunol*. 2010;184(10):5562–70.
- Pfeilstocker M, Tuechler H, Sanz G, Schanz J, Garcia-Manero G, Sole F, et al. Time-dependent changes in mortality and transformation risk in MDS. *Blood*. 2016;128(7):902–10.
- Arber DA, Orazi A, Hasserjian R, et al. The 2016 revision to the World Health Organization classification of myeloid neoplasms and acute leukemia. *Blood*. 2016;127(20):2391–2405. *Blood*. 2016;128(3):462–3.
- Cao XN, Kong Y, Song Y, Shi MM, Zhao HY, Wen Q, et al. Impairment of bone marrow endothelial progenitor cells in acute graft-versus-host disease patients after allotransplant. *Br J Haematol*. 2018;182(6):870–86.
- Kong Y, Cao XN, Zhang XH, Shi MM, Lai YY, Wang Y, et al. Atorvastatin enhances bone marrow endothelial cell function in corticosteroid-resistant immune thrombocytopenia patients. *Blood*. 2018;131(11):1219–33.
- Dight J, Zhao J, Styke C, Khosrotehrani K, Patel J. Resident vascular endothelial progenitor definition and function: the age of reckoning. *Angiogenesis*. 2022;25(1):15–33.



42. Asahara T, Murohara T, Sullivan A, Silver M, van der Zee R, Li T, et al. Isolation of putative progenitor endothelial cells for angiogenesis. *Science*. 1997;275(5302):964–7.
43. Zhao HY, Zhang YY, Xing T, Tang SQ, Wen Q, Lyu ZS, et al. M2 macrophages, but not M1 macrophages, support megakaryopoiesis by upregulating PI3K-AKT pathway activity. *Signal Transduct Target Ther*. 2021;6(1):234.
44. Tang SQ, Yao WL, Wang YZ, Zhang YY, Zhao HY, Wen Q, et al. Improved function and balance in T cell modulation by endothelial cells in young people. *Clin Exp Immunol*. 2021;206(2):196–207.
45. Hatfield K, Rynningen A, Corbascio M, Bruserud O. Microvascular endothelial cells increase proliferation and inhibit apoptosis of native human acute myelogenous leukemia blasts. *Int J Cancer*. 2006;119(10):2313–21.
46. Wen Q, Kong Y, Zhao HY, Zhang YY, Han TT, Wang Y, et al. G-CSF-induced macrophage polarization and mobilization may prevent acute graft-versus-host disease after allogeneic hematopoietic stem cell transplantation. *Bone Marrow Transplant*. 2019;54(9):1419–33.
47. Yao WL, Wen Q, Zhao HY, Tang SQ, Zhang YY, Wang Y, et al. Different subsets of haematopoietic cells and immune cells in bone marrow between young and older donors. *Clin Exp Immunol*. 2021;203(1):137–49.
48. Kong Y, Wang YT, Cao XN, Song Y, Chen YH, Sun YQ, et al. Aberrant T cell responses in the bone marrow microenvironment of patients with poor graft function after allogeneic hematopoietic stem cell transplantation. *J Transl Med*. 2017;15(1):57.
49. Song Y, Shi MM, Zhang YY, Mo XD, Wang Y, Zhang XH, et al. Abnormalities of the bone marrow immune microenvironment in patients with prolonged isolated thrombocytopenia after allogeneic hematopoietic stem cell transplantation. *Biol Blood Marrow Transplant*. 2017;23(6):906–12.
50. Subramanian A, Tamayo P, Mootha VK, Mukherjee S, Ebert BL, Gillette MA, et al. Gene set enrichment analysis: a knowledge-based approach for interpreting genome-wide expression profiles. *Proc Natl Acad Sci USA*. 2005;102(43):15545–50.
51. Pitt LA, Tikhonova AN, Hu H, Trimarchi T, King B, Gong Y, et al. CXCL12-producing vascular endothelial niches control acute T cell leukemia maintenance. *Cancer Cell*. 2015;27(6):755–68.
52. Smolich BD, Yuen HA, West KA, Giles FJ, Albitar M, Cherrington JM. The antiangiogenic protein kinase inhibitors SU5416 and SU6668 inhibit the SCF receptor (c-kit) in a human myeloid leukemia cell line and in acute myeloid leukemia blasts. *Blood*. 2001;97(5):1413–21.
53. Poulos MG, Ramalingam P, Gutkin MC, Kleppe M, Ginsberg M, Crowley MJP, et al. Endothelial-specific inhibition of NF-kappaB enhances functional haematopoiesis. *Nat Commun*. 2016;7:13829.
54. Yang M, Li J, Gu P, Fan X. The application of nanoparticles in cancer immunotherapy: Targeting tumor microenvironment. *Bioact Mater*. 2021;6(7):1973–87.
55. Agur T, Wedel J, Bose S, Sahankumari AGP, Goodman D, Kong SW, et al. Inhibition of mevalonate metabolism by statins augments the immunoregulatory phenotype of vascular endothelial cells and inhibits the costimulation of CD4(+) T cells. *Am J Transplant*. 2021;22:947–54.
56. Zhu D, Tang Q, Yu B, Meng M, Liu W, Li J, et al. Major histocompatibility complexes are up-regulated in glomerular endothelial cells via activation of c-Jun N-terminal kinase in 5/6 nephrectomy mice. *Br J Pharmacol*. 2020;177(22):5131–47.
57. Della Porta MG, Malcovati L, Rigolin GM, Rosti V, Bonetti E, Travaglini E, et al. Immunophenotypic, cytogenetic and functional characterization of circulating endothelial cells in myelodysplastic syndromes. *Leukemia*. 2008;22(3):530–7.
58. Pruneri G, Bertolini F, Soligo D, Carboni N, Cortezi A, Ferrucci PF, et al. Angiogenesis in myelodysplastic syndromes. *Br J Cancer*. 1999;81(8):1398–401.
59. Aguayo A, Kantarjian H, Manshour T, Gidel C, Estey E, Thomas D, et al. Angiogenesis in acute and chronic leukemias and myelodysplastic syndromes. *Blood*. 2000;96(6):2240–5.
60. Lundberg LG, Hellstrom-Lindberg E, Kanter-Lewensohn L, Lerner R, Palmblad J. Angiogenesis in relation to clinical stage, apoptosis and prognostic score in myelodysplastic syndromes. *Leuk Res*. 2006;30(3):247–53.
61. Alexandrakis MG, Passam FH, Pappa CA, Sfiridaki K, Tsirakis G, Damilakis J, et al. Relation between bone marrow angiogenesis and serum levels of angiogenin in patients with myelodysplastic syndromes. *Leuk Res*. 2005;29(1):41–6.
62. Kong Y, Wang Y, Zhang YY, Shi MM, Mo XD, Sun YQ, et al. Prophylactic oral NAC reduced poor hematopoietic reconstitution by improving endothelial cells after haploidentical transplantation. *Blood Adv*. 2019;3(8):1303–17.
63. Wang Y, Kong Y, Zhao HY, Zhang YY, Wang YZ, Xu LP, et al. Prophylactic NAC promoted hematopoietic reconstitution by improving endothelial cells after haploidentical HSCT: a phase 3, open-label randomized trial. *BMC Med*. 2022.
64. Raaijmakers MH, Mukherjee S, Guo S, Zhang S, Kobayashi T, Schoonmaker JA, et al. Bone progenitor dysfunction induces myelodysplasia and secondary leukaemia. *Nature*. 2010;464(7290):852–7.
65. Walkley CR, Shea JM, Sims NA, Purton LE, Orkin SH. Rb regulates interactions between hematopoietic stem cells and their bone marrow microenvironment. *Cell*. 2007;129(6):1081–95.

## Publisher's Note

Springer Nature remains neutral with regard to jurisdictional claims in published maps and institutional affiliations.

**Ready to submit your research? Choose BMC and benefit from:**

- fast, convenient online submission
- thorough peer review by experienced researchers in your field
- rapid publication on acceptance
- support for research data, including large and complex data types
- gold Open Access which fosters wider collaboration and increased citations
- maximum visibility for your research: over 100M website views per year

**At BMC, research is always in progress.**

Learn more [biomedcentral.com/submissions](https://biomedcentral.com/submissions)

